Beam Scanning Comb-Line Antenna Loading Movable Dielectric Plate

Kazuhiro Kitatani, Takahiko Terada and Yasuyuki Okamura
Graduate School of Engineering Science, Osaka University
1-3 Machikaneyama, Toyonaka, Osaka, 560-8531 Japan
E-mail: kitatani@ee.es.osaka-u.ac.jp, okamura@ee.es.osaka-u.ac.jp

Abstract

This paper describes a beam scanning antenna loading a movable dielectric plate on a microstrip comb-line antenna. This antenna uses the mechanical system that has the characteristic of an easy structure as well as low costs. The comb, a radiation element, is connected to a microstrip line. The beam direction of the proposed antenna changes according to phase shifts of the microstrip line moving the loaded dielectric plate. First, a guide wavelength change at quasi-millimeter wave band (20GHz) was measured when moving the dielectric plate loaded on the microstrip line. The possibility of the beam scan of the antenna is shown. Next, the comb-line antenna was fabricated and the antenna characteristics were measured. A possible beam scanning angle of 20 degrees was confirmed by moving the plate.

1. INTRODUCTION

A microstrip antenna [1] with compactness and lightness has been used in various radio communication systems such as mobile communications like an airplane and a car. Recently, the development of ITS technology, Intelligent Transport Systems, has been advanced. The research of the beam scanning antenna for the car radar of the millimeter wave using a mechanical and movable system is paid to attention. A waveguide [2],[3], an NRD guide, NonRadiative Dielectric guide [4], and a microstrip line [5] have been used up to now as a feeding line of an array antenna, and the beam scanning has achieved the phase change by movement with the actuator mechanically by arranging the dielectric and the metal on the feeding line. These antennas are different from the type that moves the radar itself used in the airlane watch radar and the ship radar. The response time of such antennas becomes about milli-second, and they are excellent in loss, cost and power consumption compared with those made of a semiconductor. Also, antennas using MEMS (Micro-Electro-Mechanical-Systems) technology have been actively researched [6].

We have been advancing the development of antennas for the millimetre wave car radar. In this paper, the beam scanning antenna loading a movable dielectric plate on a microstrip comb-line antenna [7] is demonstrated. The principle of the operation of the proposed antenna, the design in the quasi-millimeter wave band, and the experimental results of the fabricated antenna are described in detail.

2. OPERATION AND STRUCTURE OF AN ANTENNA

Figure 1 shows a schematic configuration of the proposed antenna. This antenna has a structure in which a dielectric plate is loaded on the upper part of the comb-line antenna. Combs, radiation elements, are periodically arranged on the microstrip line in Fig.1 (a). Figure 1(b) is a detailed portion of the comb and the dielectric plate. The comb-line antenna has little loss due to the structure connecting the radiation element to the microstrip line directly [8]. In Fig. 1 (a), the dielectric plate can be slid in the direction of the *y*-axis. The propagation wavelength of the microstrip line can be changed, thus the scan of the antenna main beam is attainable by changing of the phase between the radiation elements.

First, the comb-line antenna when not loading the dielectric plate was designed using a simulation software, S-NAP/Field. An operation frequency was set to be 20GHz and the main beam was inclined about +10 degrees, about 100 degrees in the θ direction, from the broadside.

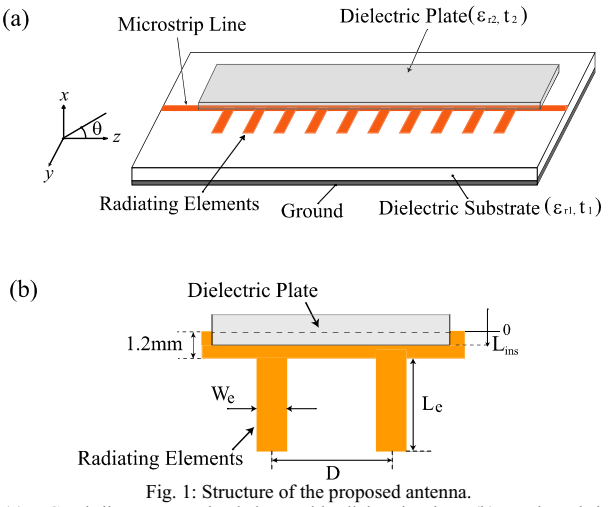

Fig. 1: Structure of the proposed antenna.
(a) Comb-line antenna loaded movable dielectric plate, (b) comb and the dielectric plate.

The dielectric substrate has a relative permittivity (ε_{r1}) of 2.2 and a thickness (t_1) of 0.4mm. The parameters of the antenna element were an element interval D of 9.8mm, a comb width W_e of 3mm, and a comb length L_e of 4.8mm. The line width W of the microstrip line was 1.2mm (a characteristic impedance: 50Ω), and the wavelength compaction ratio ζ was set to 0.723. $\zeta=\lambda_g/\lambda_0$ defines the wavelength compaction ratio. λ_g is the propagation wavelength of the microstrip line, and λ_0 is the free-space wavelength. Here, the radiation element was assumed to be a point source model for the calculation. The direction θ_m of the main beam is given by the following equation,

$$\theta_m = \cos^{-1}[\frac{1}{D}(\frac{D-2d_1}{\zeta}-\lambda_0)] \qquad (1)$$

d_1 is the correction length caused by the influence of the T-junction of the microstrip line and the radiation element. d_1 is given by the following equation,

$$d_1 = \frac{0.02W_e}{2(1-0.02W_e)}D \qquad (2)$$

The relation between the direction of the main beam and the wavelength compaction ratio of the microstrip line was calculated using eqs. (1) and (2) for λ_0=15mm. The result is shown in Fig. 2. In order to obtain the beam scan of ±10 degrees in the direction of the broadside, the wavelength compaction ratio of 0.56 to 0.72 is needed. The correction length d_1 of the element interval was about 0.3mm. Next, the method to change the wavelength compaction ratio is described.

Figure 3 shows the cross-sectional structure of the microstrip line loading a dielectric plate. The wavelength compaction ratio of the microstrip line was calculated using the variational method [9] for a relative permittivity (ε_{r2}) of 4 to 10, and a thickness (t_2) of 0 to 1.0mm. The result is shown in Fig. 4. The wavelength compaction ratio of the microstrip line was set to 0.723 without the dielectric over-plate. When the relative permittivity of the dielectric plate increases, the wavelength compaction ratio decreases. Also, the wavelength compaction ratio is the similar change when the thickness of the dielectric plate increases. The wavelength compaction ratio of 0.56 is required for obtaining the scanning angle of 20 degrees. The dielectric plate with the relative permittivity (ε_{r2}) of about 10, and the thickness (t_2) of 0.6mm or more is suitable. Therefore, we used the alumina substrate (ε_{r2}=9.8, t_2=0.8mm and $\tan\delta=1\times10^{-4}$) as the actual dielectric plate.

The wavelength compaction ratio was measured using a conventional network analyzer (H.P-8510C). First, the wavelength compaction ratio of the microstrip line without the dielectric over-plate was measured using the TDR (Time Domain Reflectometry) method. The straight microstrip line on 50Ω of a length of 190mm was fabricated. The small discontinuities on the microstrip line, a width of 2mm and a length of 0.5mm, were attached in the interval of 150mm length. The wavelength compaction ratio of 0.721 was measured from the delay time, 1.3878nsec, for 150mm length. This is well in agreement with the prediction: 0.723. Next, the wavelength compaction ratio of the microstrip line with the movable dielectric plate was measured from the phase shifts of the transmission characteristics (S_{21}). The alumina substrate, a length of 95mm, a width of 20mm, was used as the dielectric plate. The microstrip line was a length of 150mm. The dielectric plate was moved by a linear actuator. The measured results of the wavelength compaction ratio when changing the insertion length of the dielectric plate is shown in Fig. 5. The edge of the microstrip line was set to L_{ins}=0mm. The phase change did not appear for L_{ins}=-1mm, and the wavelength compaction ratio was 0.721. When the dielectric plate was moved to the other edge of the microstrip line, the wavelength compaction ratio gradually changed by the fringing effect. The edge of the microstrip line had a large electric field, and the wavelength compaction ratio showed a large change in little movement. In this case, the wavelength compaction ratio was achieved from 0.563 to 0.724 for the insertion length of 4mm to -1mm. Therefore, the main beam of the antenna can be continuously scanned about 20 degrees.

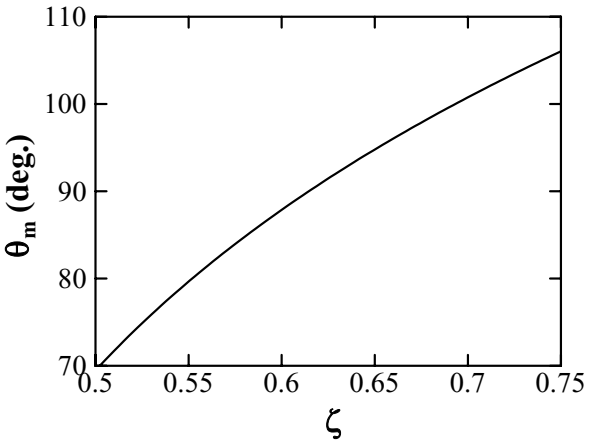

Fig. 2: Relation between the direction of the main beam (θ_m) and the wavelength compaction ratio (ζ) of the microstrip line.

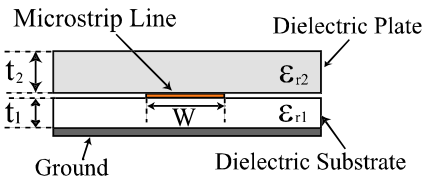

Fig. 3: Structure of the microstrip line loading a dielectric plate. (Microstrip line parameters are : ε_{r1}=2.2, t_1=0.4mm, and W=1.2mm, dielectric plate parameters : ε_{r2} and t_2)

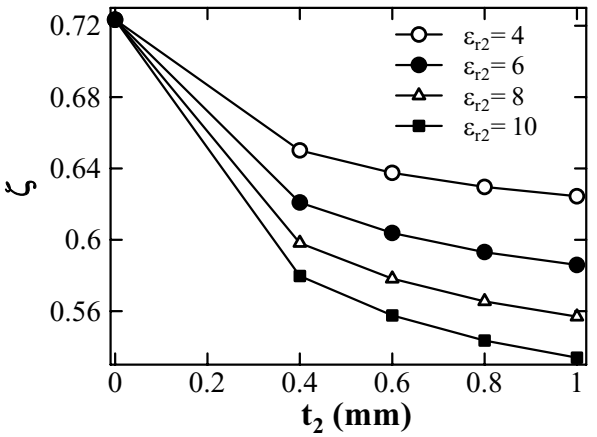

Fig. 4: The wavelength compaction ratio (ζ) of microstrip line when changing as for a relative permittivity (ε_{r2}) and thickness (t_2).

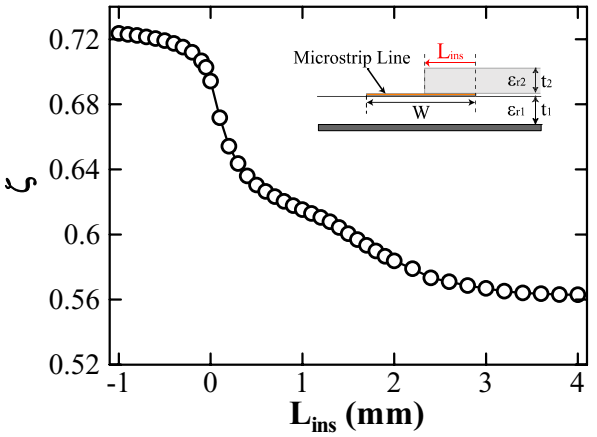

Fig. 5: The measurement results of the wavelength compaction ratio when changing the insertion length (L_{ins}) of the dielectric plate.

3. EXPERIMENT RESULTS

The antenna operating at 20GHz was fabricated to confirm the proposal. The radiation and the impedance characteristics of the antenna were measured. The number of antenna elements was 10, and each parameter of the antenna was used from the simulation results. The printed circuit board used a fluorocarbon-resin substrate (ε_{r1}=2.2); the size was 150 × 60 × 0.4mm^3 and the copper thin film was 18μm. The size of the dielectric plate of the alumina substrate was 120 × 20 × 0.8mm^3. The SMA connector was arranged in the input and output parts of the antenna. The termination of 50Ω was attached in the output part. The alumina plate was moved with the linear actuator, controlled with the microcomputer.

A. Radiation characteristics

We measured the radiation pattern of the fabricated antennas. H-plane (*zx*-plane) patterns at 20GHz for L_{ins}=-1mm and L_{ins}=4mm are shown in Figs. 6 and 7, respectively. Those antennas are operating as an H-plane array. Fig. 7 is the case where the dielectric plate was loaded in the whole area of the antenna. The main beam of the antenna was 103.2 degrees for L_{ins}=-1mm and 83.2 degrees for L_{ins}=4mm. The possible beam scanning angle of 20 degrees was confirmed by moving the plate. In the figures, the plot of the dotted lines shows the calculated results. The direction of the main beam was 104.1 degrees for L_{ins}=-1mm, and 80.9 degrees for L_{ins}=4mm, the results of which were well in agreement with the experimental results.

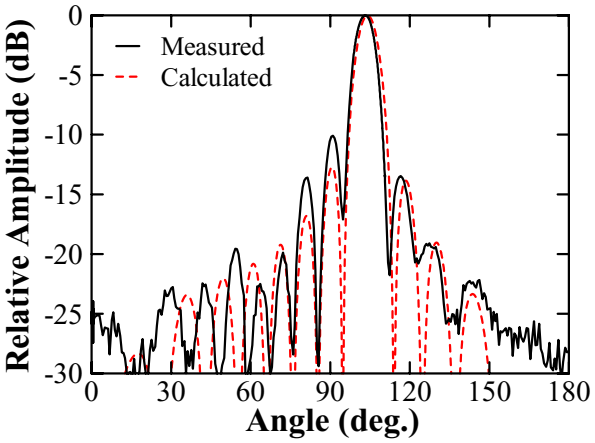

Fig. 6: H-plane (*zx*-plane) pattern at 20GHz, L_{ins}=-1mm.

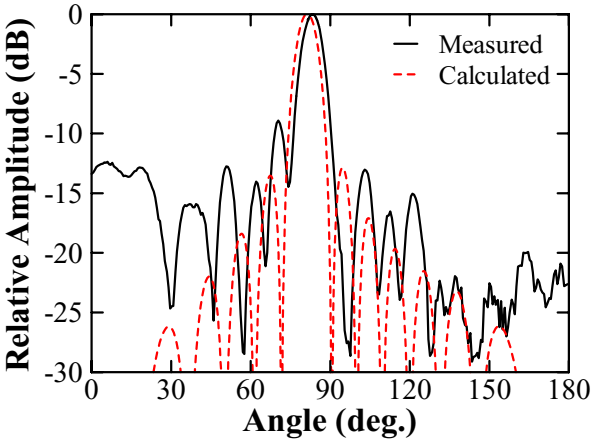

Fig. 7: H-plane (*zx*-plane) pattern at 20GHz, L_{ins}=4mm.

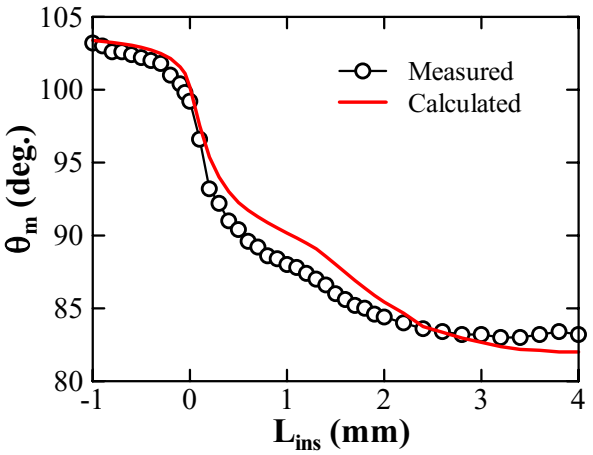

Fig. 8: Relation between the direction of the main beam (θ_m) and the insertion length (L_{ins}) of the dielectric plate.

Figure 8 shows the measured main beam direction as a function of the insertion length of the dielectric over-plate. To compare with the measured result, the calculated result is also plotted using the wavelength compaction ratio in Fig.5. The main beam of the antenna can be continuously scanned by changing the insertion length L_{ins}. They were fairly in agreement.

Next, the radiation patterns of the H-plane, the E-plane (*xy*-plane) and the cross polarization ingredients are shown in Fig. 9. The main beam was a broadside direction when the insertion length of the dielectric plate was L_{ins}=0.5mm. The E-plane showed an unsymmetrical pattern with the peak direction of near 80 degrees and showed wavy by the influence of the ground. The amplitude at the direction of the front was 1.8dB down from the peak value. The maximum value of the cross polarization ingredient was -10.5dB for the E-cross and was -13.4dB for the H-cross. The side lobe level of the H-plane was -11dB. Moreover, the 3dB beam width of the H-plane was 7.4 degrees to 8.4 degrees. The side lobe level and the cross polarization ingredient should to be decreased for the actual application.

Figure 10 shows the relation between the measured absolute gain and the insertion length. The gain of the antenna lies between 10.1dBi and 12.7dBi. We can notice a large dip near the insertion length of 1mm. The position at which the change occurred corresponds to the appearance of the comb. This point is considered to be the cause such as the influence of the reflection by the end of the dielectric plate and the reduction of the current on the comb. We examined the dip based on the experimental result of the following impedance characteristics.

B. Impedance characteristics

The return loss and the transmission loss of the antenna were measured using the network analyzer. Figure 11 shows the reflection characteristics. L_{ins} were -1mm, 1.2mm, 2mm, and 4mm. The measured frequency range was 18-22GHz. The worst return loss was observed at the frequency of 19GHz for L_{ins}=4mm, but other cases were less than -10dB. Thus, the fabricated antenna can be matched in the broadband.

Figure 12 shows the relation between the insertion length and the transmission loss ($|S_{21}|$) and the return loss ($|S_{11}|$) at 20GHz. When the dielectric plate was moved from -1mm to the microstrip line, the reflection increased. The return loss became the largest value of -11dB at the position where the plate was wholly attached to the comb. The reflection decreased as the dielectric was inserted further. The result indicates that the reflection attributes to the gain decrease in Fig.10. When setting the insertion length to -1 to 1.2mm, $|S_{21}|$ was about -5dB. However, the transmission and the reflection decreased as the dielectric plate moved from L_{ins}=1.2mm to the outer region, which is caused by the radiation.

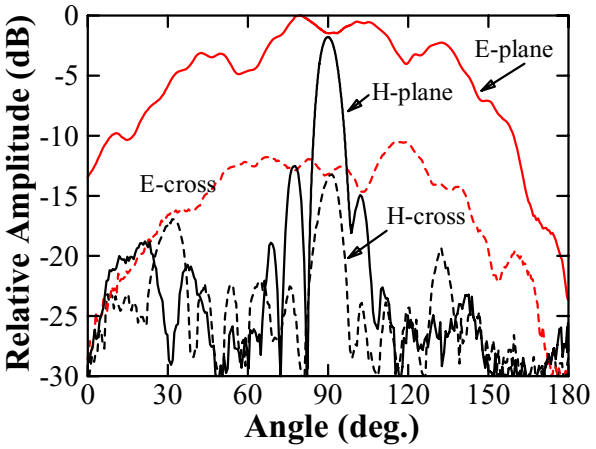

Fig. 9: Radiation patterns at 20GHz, L_{ins}=0.5mm
H-plane and the E-plane (*xy*-plane), and the cross polarization ingredient.

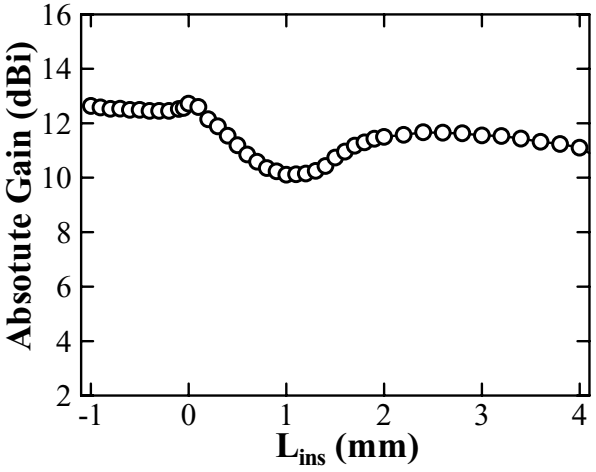

Fig. 10: Relation between the absolute gain of the front direction (*z*-direction) and insertion length.

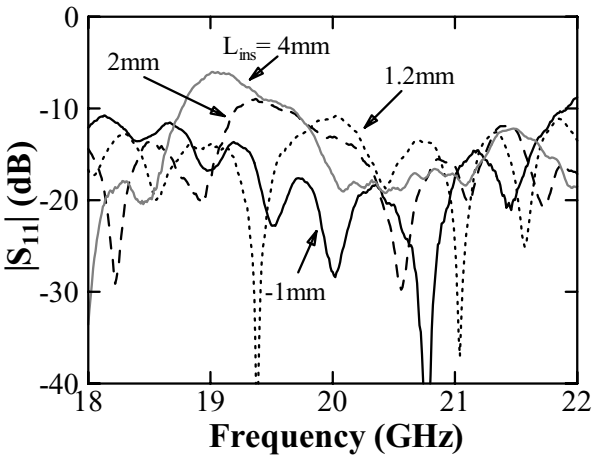

Fig. 11: Return loss of the proposed antenna. (L_{ins} were -1mm, 1.2mm, 2mm and 4mm)

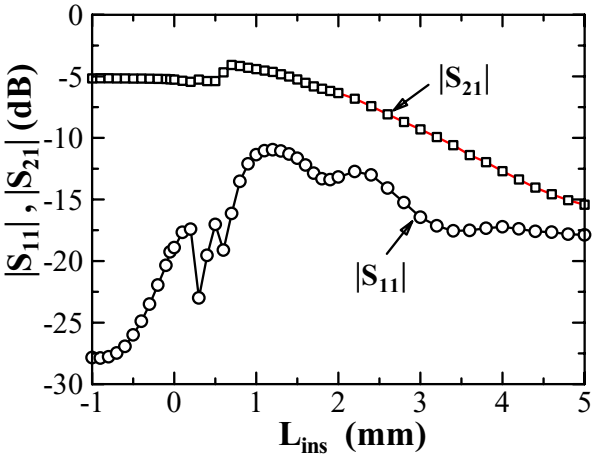

Fig. 12: Transmission loss $|S_{21}|$ and $|S_{11}|$ at 20GHz when changing insertion length.

C. Discussion

Here, the H-plane cross polarization ingredient of the antenna is examined. Figure 13 shows the relation between the measured cross polarization ingredient of the H-plane and the insertion length of the dielectric plate. A vertical axis was normalized with the maximum value of the H-plane receiving amplitude. The cross polarization ingredient of the H-plane was increased as the insertion length of dielectric plate increased. When the insertion length was small, the current on the comb was dominant in the direction of *y*-axis. When the dielectric plate was deeply inserted in the comb, the current distribution of the comb changed and ingredients other than the *y*-axis was produced. When the insertion length was 5.4mm, the H-plane and the cross polarization ingredient were nearly the same. This indicates that the circularly polarized wave can be generated. The pattern of the antenna was measured accordingly. The result is shown in Fig. 14. Although the axial ratio was as large as 3.2dB, the radiation of circularly polarized wave was observed. The discrepancy is because there existed the difference in the receiving level in 45 degrees from the *y* direction even though the amplitudes in the *y*-direction and the *z*-direction were the same.

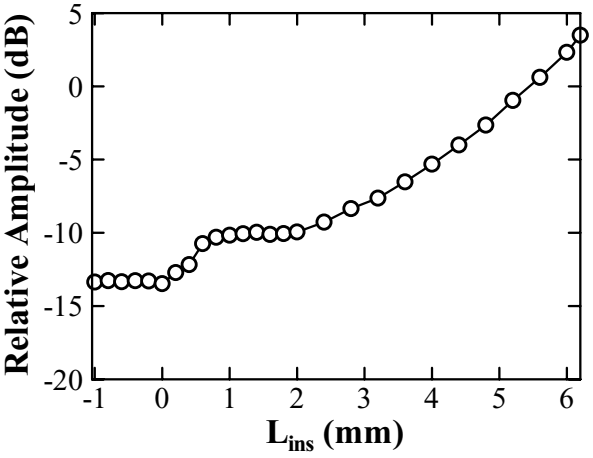

Fig. 13: Relation between the H-plane cross polarization ingredient and insertion length.

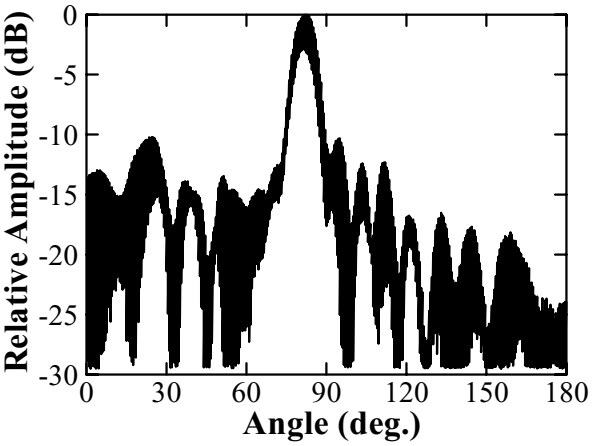

Fig. 14: Radiation pattern of L_{ins}=5.4mm.

4. CONCLUTION

This paper presents the comb-line antenna loaded the movable dielectric board aiming at the application to the antenna for millimeter wave car radars. The principle of the beam scanning operation of the antenna was described and the antenna operating at the quasi-millimeter wave band was designed. First, the change in the guide wavelength at the quasi-millimeter wave band (20GHz) was measured when

moving the dielectric plate loaded on the microstrip line. The possibility of the beam scan of the antenna was shown. Next, the proposed antennas were fabricated and demonstrated. The beam scanning angle of 20 degrees was confirmed by moving the plate using the liner actuator, although the radiation pattern had an unwanted large side lobe level and cross polarization ingredient. Furthermore, we discovered the possibility of the circular polarization wave generation when the insertion position of the dielectric plate was properly chosen.

ACKNOWLEDGEMENT

We would like to thank Emeritus Prof. S. Yamamoto and Dr. S. Nishimura for their constant encouragement. We also thank Toyota Central R&D Labs., Inc. and the Osaka University central workshop.

REFERENCES

[1] K.F.Lee, and W.Chen, "Advances in microstrip and printed antennas, " John Wiley& Sons, Inc., 1997.

[2] M.Higaki, J.Hirokawa and M.Ando, "Mechanical phase shifting in the power divider for single-layer slotted waveguide," IEICE Trans. Commun., vol. E87-B, no.2, pp.310-316, Feb. 2004.

[3] T.Kondo, J.Hirokawa, K.Sakurai and M.Ando, "Feasibility of mechanical beam scan by movable dielectric blocks in the feeder of a single-layer waveguide array antenna," IEICE Electronics Express, vol.3, no.2, pp.29-33, Jan. 2006.

[4] Y.Wagatsuma, Y.Daicho, O.Kuboyama, T.Yanagisawa and T.Yoneyama, "Beam scanning car waning radar using NRD," IEICE Electronics Society Conference, SC-2-9, pp.283-284, 1999.

[5] S.Matsuzawa, K.Sato, Y.Inoue and T.Nomura, "W-band steerable composite right/left-handed leaky wave," IEICE Gen. Conf, B-1-61, 2006.

[6] V.K.Varadan, K.J.Vinoly and K.A.Jose, "RF MEMS and their applications," John Wiley Sons Ltd., 2003.

[7] K.Kitatani, T.Terada and Y.Okamura, "The beam scanning characteristics of comb line array antenna loaded with dielectric plate," IEICE Gen. Conf, B-1-44, 2006.

[8] J.R.James and P.S.Hall, "Handbook of microstrip antennas," IEE Electromagnetic Waves, Peter Pereginus, London, Series 28, 1989.

[9] E. Yamashita, "Variational method for the analysis of microstrip-like trans-mission lines," IEEE Trans. on Microwave Theory and Tech., vol.16, no.8, pp.529-535, August 1968.